Phase-space-density limitation in laser cooling without spontaneous emission

Thierry Chanelière,[1,2] Daniel Comparat,[1] and Hans Lignier[1]
[1]*Laboratoire Aimé Cotton, CNRS, Univ. Paris-Sud, ENS Paris Saclay, Université Paris-Saclay, Bât. 505, 91405 Orsay, France*
[2]*Univ. Grenoble Alpes, CNRS, Grenoble INP, Institut Néel, 38000 Grenoble, France*

(Received 14 June 2018; published 27 December 2018)

We study the possibility to enhance the phase-space density of noninteracting particles submitted to a classical laser field without spontaneous emission. We clearly state that, when no spontaneous emission is present, a quantum description of the particle motion is more reliable than semiclassical description, which can lead to large errors especially if no care is taken to smooth structures smaller than the Heisenberg uncertainty principle. Whatever the definition of position-momentum phase-space density, its gain is severely bounded especially when started from a thermal sample. More precisely, the maximum of the position-momentum phase-space density can only increase by a factor M for M-level particles. This bound comes from a transfer between the external and internal degrees of freedom. Therefore, it is impossible to increase the position-momentum phase-space density in the same internal state.

DOI: 10.1103/PhysRevA.98.063432

I. INTRODUCTION

It is usually believed that the phase-space density (PSD) of noninteracting particles cannot be increased by using only pure Hamiltonian evolution and any PSD increase would require a dissipative mechanism [1,2]. In the context of laser cooling, this dissipation is usually ensured by spontaneous emission. Nevertheless, in recent years, several papers suggested that some experimental observations could support the possibility of an optical cooling without spontaneous emission [3–5]. These counterintuitive results were also supported by theoretical arguments and semiclassical simulations using classical laser fields [6–8]. The perspective of cooling different species including molecules has actively stimulated the discussions [9–11].

In this paper, we specifically address the issue of increasing the PSD for noninteracting particles submitted to classical laser fields (i.e., equivalent to quantum fields in coherent mode [12–14]) and deprived of spontaneous emission. We first determine the evolution of a position-momentum distribution (PMD) of such particles (often called atoms hereafter even though molecules are also concerned) in a phase-space region. In particular, we show that a quantum treatment of the external degrees of freedom is more reliable than a classical treatment that may lead to erroneous predictions. A quantum description of position and momentum requires one to revisit the definition of the classical PMD, to define quantum analogs, and to discuss their characterizations. Because the term "cooling" is ambiguous and has often led to misinterpretations and controversies, we perform our analysis by considering both the PMD and several definitions of a single quantity (rather than a distribution) called PSD in a generic way. Somehow, the most straightforward definition of PSD is the maximum of PMD. Other definitions, such as those derived from different entropies, are used to account for the populations and correlations of the internal and external degrees of freedom. With these careful definitions, we establish that PSD can marginally increase in the case of an initial thermal distribution. Yet the gain is shown to be bounded by the number M of internal levels.

First of all, it is important to recall that the evolution of noninteracting particles can be derived from a single-particle statistics. In this framework, we do not study single realizations of many-particle evolution that may cause PMD modification driven by ergodicity, Zermelo-Poincaré recurrence, or fluctuation theorems [15] as through coarse-grained PMD [16,17] or by phase-space volume surrounding particles (such as ellipsoid emittance growth in beams) [18]. Therefore, we assume the ensemble evolution as entirely derived from the one-particle density matrix $\hat{\rho}$ in the quantum case and, in the classical case, from the (statistical averaged single-particle) classical PMD $\rho(\boldsymbol{r}, \boldsymbol{v}, t)$.

The most general evolution of the classical PMD undergoing a (nonrandom) external force $\boldsymbol{F}(\boldsymbol{r}, \boldsymbol{v}, t)$ is given by the continuity equation:

$$\frac{D\rho}{Dt} = \frac{\partial\rho}{\partial t} + \left(\boldsymbol{v}\cdot\frac{\partial}{\partial\boldsymbol{r}}\right)\rho + \frac{\boldsymbol{F}}{m}\cdot\frac{\partial\rho}{\partial\boldsymbol{v}} = -\rho\frac{\partial}{\partial\boldsymbol{v}}\cdot\frac{\boldsymbol{F}}{m}, \quad (1)$$

where $\frac{D\rho}{Dt}$ is the material derivative. This clearly shows that a velocity-dependent force is necessary to change the PMD ρ. The Doppler cooling scheme, using for example the classical Lorentz oscillator model, is a textbook example of velocity-dependent force. However, in Hamiltonian mechanics, according to the Vlasov-Liouville theorem $\frac{D\rho}{Dt} = 0$ for noninteracting particles, ρ is constant. This is consistent with the continuity equation because friction forces cannot be included in our closed system with external fields.[1] Since quantum mechanics is also based on a Hamiltonian description, one may wonder how the maximum of a PMD could be increased.

[1]For example, an electric charge submitted to the Lorentz force $\boldsymbol{F} = q(\boldsymbol{E} + \boldsymbol{v}\times\boldsymbol{B})$ verifies $\frac{\partial}{\partial\boldsymbol{v}}\cdot\boldsymbol{F} = 0$.

A major difference actually comes from the treatment of the internal degrees of freedom that cannot be rigorous in classical physics. Regarding the electromagnetic interactions, the time evolution of the internal degrees of freedom is generally calculated by the quantum master equation acting on the density matrix because it may also include nonunitary evolutions due to spontaneous emission. The semiclassical evolution of the external degrees of freedom is then usually obtained by Ehrenfest's theorem. This framework provides satisfying predictions for Doppler cooling where the change of semiclassical PMD maximum is essentially attributed to spontaneous emission. However, even without spontaneous emission, several semiclassical studies suggest that the maximum of a PMD can be modified [π pulse, rapid adiabatic passage (RAP), stimulated RAP, and bichromatic fields [3,5,6,8,10]]. Their common idea is that a coherent force, resulting from absorption and stimulated emissions, depends on the particle velocity via the Doppler effect. So a large increase of the PMD maximum seems possible from the continuity equation (1). In the following, we will show that the concept of semiclassical force is only partly correct and that the Ehrenfest's theorem can lead to an important overestimation of the cooling efficiency. We will show that a proper quantum-mechanical treatment exhibits a limited gain in the PMD, its maximum being the number M of internal levels.

II. INCREASING THE POSITION-MOMENTUM DISTRIBUTION

A. Basic mechanism

The basic physical mechanism and maximum gain of PMD can be understood using an ensemble of noninteracting two-level atoms (with ground $|g\rangle$ and excited $|e\rangle$ internal states) and momentum states $|\boldsymbol{p}\rangle$. Because the atoms do not interact with each other and do not undergo spontaneous emission, as discussed in detail in Appendix A, the one-particle Hamiltonian where the fields are classical [Eq. (A2)] is sufficient to describe the dynamics. We ran several simulations based on various optical schemes, including bichromatic fields, rapid adiabatic transfers, and π pulses. In all cases, we found the same limitations on the gain of the PMD maximum. The underlying reasons can be understood with the example sketched in Fig. 1. It shows how a light pulse (with Doppler detuning and Rabi frequency Ω wisely adjusted to address a narrow line recoil transition) may bring two atoms in the same momentum state $|\boldsymbol{p}\rangle$, while the internal state of the displaced atom is changed. Any attempt to increase further the population of $|\boldsymbol{p}\rangle$ is vain because the rates of absorption and stimulated emission are equal, which prevents increasing the population in $|\boldsymbol{p}\rangle$. This qualitatively explains the limited gain in position-momentum PSD gain by a factor 2 for two-level atoms.

B. Evolutions

We now confirm this limitation by accurate calculations for two pulses in one dimension as depicted in Fig. 1. The classical evolution and the quantum evolution of an initial two-dimensional (thermal) Gaussian PMD in (r, p) are given

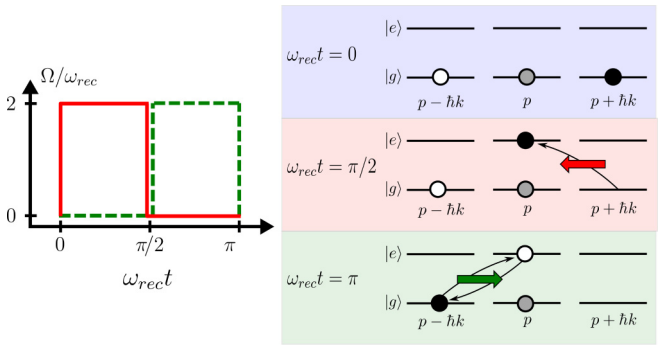

FIG. 1. Left: pulse sequence, a π pulse coming from the right (red) followed by a π pulse coming from the left (green). Right: basic idea of PMD maximum increase. The first π pulse transfers one atom from $|p + \hbar k, g\rangle$ to $|p, e\rangle$ without affecting the atom already in state $|p, g\rangle$, thereby increasing the total number of particles in $|p\rangle$ by a factor 2. Trying to add a third particle in the same momentum $|p\rangle$ cell, by applying a second π pulse counterpropagating, simply swaps the particles in each state with no gain in $|p\rangle$ population. $\omega_{\rm rec} = \hbar k^2/2m$ and Ω are the recoil and Rabi frequencies, respectively.

in Fig. 2. The quantum evolution is based on the density-matrix master equation $\hat{\rho}(r, p, t)$ as defined in Appendix A 4 a following Eq. (A12) and the Wigner function $W(r, p, t)$ as defined in Appendix A 4 b following Eqs. (A13)–(A15). The semiclassical evolution makes use of Newton's equation of motion with a force defined Eq. (B9) resulting from the Ehrenfest theorem and Bloch equations using the $\hbar k \to 0$ limit of the Wigner quantum evolution (see Appendix B). The evolution of the semiclassical PMD was calculated with a billion test particles. The final distribution corresponds to the number of atoms in a position-momentum cell whose size has been arbitrarily chosen as $1/(5k)$ in position and $\hbar k/10$ in momentum. In these conditions, the maximum of the semiclassical PMD is subject to a large gain (factor 20), which significantly overcomes the quantum approaches where the maximum gain of the Wigner PMD reaches 2.5. The semiclassical approach should indeed be handled with precaution to predict the PMD evolution. When spontaneous emission is present, the collapse of the atomic wave packet [19] smooths out the evolution on a time scale longer than the spontaneous emission time. Therefore, the internal variables relax fast enough and follow quasiadiabatically the slower external motion; so the evolution of the Wigner distribution is reduced to the semiclassical one as demonstrated in Appendix B 2. On the contrary, without spontaneous emission, correlations may appear between internal and external variables [20] invalidating the semiclassical approach.

C. Discussion

The physical relevance of the previous calculations have to be discussed in the light of the position-momentum uncertainty principle because both the quantum and semiclassical distributions exhibit structures smaller than the minimum uncertainty. This problem is often present in the distributions processed in cooling or brightening studies [3–5,10,11]. This issue can be solved by performing a convolution of the PMD with a Gaussian function corresponding to the Heisenberg

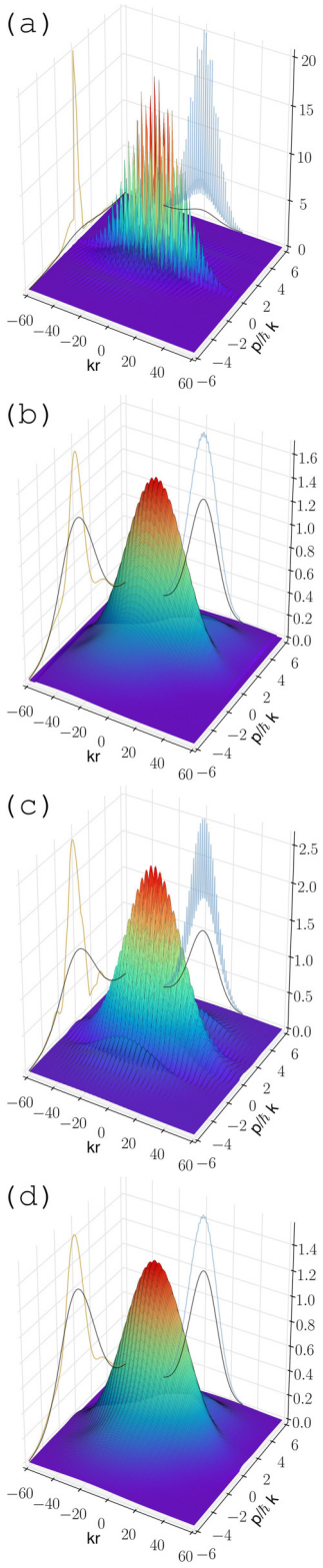

FIG. 2. PMD evolution starting with an initial Gaussian PMD (normalized to a maximum of 1 and represented by black lines on the projections). The histogram of the position-momentum semiclassical evolution for cell size of $1/(5k)$ in position and $\hbar k/10$ in momentum (a) and smoothed distribution (b) as well as the total (ground plus excited states) Wigner (c) and Husimi (d) functions are shown after a pair of π pulses (left-right) with Rabi frequency $2\omega_{\mathrm{rec}}$ and pulses detuning $-2\omega_{\mathrm{rec}}$.

limit $\sigma_r\sigma_p = \hbar/2$, which gives the smoothed coarse-grained distributions shown in Figs. 2(b) and 2(d), where we chose $k\sigma_r = \frac{\sigma_p}{\hbar k} = \frac{1}{\sqrt{2}}$. Applied to a Wigner function, we obtain the so-called $Q(r, p, t)$ Husimi distribution, which is the optimal probability distribution for joint position and momentum measurement [21]. The effect is quite striking since, in our example, the classical and quantum smoothed PMD are very similar (but still different) and both indicate a maximum gain of 2. The similitude may depend on the specificities of our toy model. Other protocols could give rise to far more significant differences. Indeed, even with a smoothing postprocedure, the semiclassical evolution should fail at the time when particles initially in the ground state and contained in a Heisenberg-bounded PSD region undergo different forces (or Rabi frequencies).

III. INCREASING THE PHASE-SPACE DENSITY

A. Definitions

In order to precisely understand the role of the interplay between internal and position-momentum degrees, we now adopt an analysis relying on the density matrix $\hat{\rho}$. For this purpose, we use the quantum PSD as a quantity linked to the entropy S (per particles and per unit of k_B) through to the Boltzmann formula

$$S = -\ln D, \tag{2}$$

where D defines the PSD quantitatively. This definition is similar to the Sackur-Tetrode formula $S = -\ln D + \frac{5}{2}$ that gives the thermal classical PSD used by the ultracold atoms community (the number of particles contained in a de Broglie's wavelength sized box reaches unity when quantum degeneration is reached). We first consider the Von Neuman entropy

$$S_{\mathrm{VN}} = -\mathrm{Tr}[\hat{\rho}\ \ln(\hat{\rho})] = -\sum_i \lambda_i \ln(\lambda_i), \tag{3}$$

where λ_i are the eigenvalues of the singleparticle density matrix $\hat{\rho}$. These eigenstates generally do not correspond to physical observables $|i\rangle$ as the energy eigenstates for example. So other quantities are commonly used, such as the informational Shanon entropy

$$S_{\mathrm{Sh}} = -\sum_i p_i \ln p_i, \tag{4}$$

where $p_i = \langle i|\hat{\rho}|i\rangle$ is the population of the ith eigenstate. Consequently, we define D_{VN} and D_{Sh} from Eq. (2). These particular cases belong to two distinct and general categories: eigenvalue-based (or spectral) entropy and population-based (or informational) entropy. The first kind is independent of the representation basis and thus invariant under Hamiltonian evolution, while the second kind depends on the representation and consequently is likely to change over time.

B. Evolutions

In these conditions, one can wonder whether a quantum entropy can decrease or not. To answer this question, we reconsider the evolution during the pair of π pulses that gave rise to the PMD in Fig. 2. However, in order to calculate

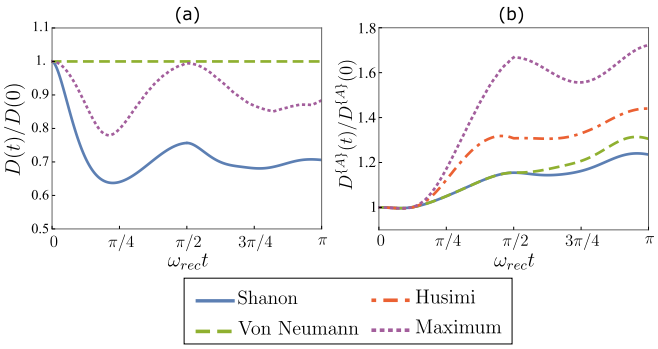

FIG. 3. Evolution of several definitions of PSD, normalized to their initial value: (Husimi, max $[\hat{\rho}]$, Von Neuman $S_{\rm VN}$, and Shanon $S_{\rm Sh}$ entropies) under same conditions as in Fig. 2 but with initial full spatial delocalization. (a) Evolution for the total (external + internal degree of freedom). (b) Only external degree of freedom (denoted A) for max $[\hat{\rho}^A]$, max $[Q^{\{A\}}]$, $D^{\{A\}}_{\rm VN}$, and $D^{\{A\}}_{\rm Sh}$ bounded by 2.

$D_{\rm Sh}$ and $D_{\rm VN}$ more easily, we now assume that the atoms are initially fully delocalized in position, which implies that the initial density matrix is Gaussian diagonal when expressed in $|p\rangle$ basis. We checked that this small modification had almost no effect on the evolution of the gain observed from the PMD (Fig. 2 shows that the smoothed spatial distribution was almost not affected by the time evolution). As expected, we see in Fig. 3(a) that the Von Neuman entropy is invariant while the Shanon entropy is not. More fundamentally, an initial thermal state provides the largest possible PSD and prohibits further PSD increase [1]. Indeed, the minimum Shanon entropy is achieved by a thermal Gaussian state [22] and then equals the Von Neuman entropy. So in our case $D_{\rm Sh}(t) \leqslant D_{\rm Sh}(0) = D_{\rm VN}(0)$. Yet it is noticeable that, unlike the Von Neumann PSD, the Shanon PSD can locally increase as observed in Fig. 3(a) between $\omega_{\rm rec}t = \pi/4$ and $\omega_{\rm rec}t = \pi/2$ when the density matrix is no longer Gaussian diagonal. Thus cooling is indeed possible if starting from nonthermal states (as the one produced at time $\omega_{\rm rec}t = \pi/4$).

C. Discussion

Finally, we would like to discuss the decrease of $D_{\rm Sh}$ and the invariance of $D_{\rm VN}$, which seems to contradict the results of Fig. 2, where all the distribution maxima increase. This apparent contradiction comes from the fact that the whole density matrix we consider is composed of two subspaces: the full atomic system AB ($\hat{\rho} = \hat{\rho}_{AB}$) is formed by the external degrees of freedom (part A) and the M internal degrees of freedom B (here $M = 2$). As the PMD in Fig. 2 are functions of the coordinates (r, p) (part A), it is thus more appropriate to evaluate $S^{\{A\}}$ (or $D^{\{A\}}$), i.e., S (or D) restricted to A by using the partial trace over the internal degrees of freedom $\hat{\rho}_A = {\rm Tr}_B\hat{\rho}$ instead of $\hat{\rho}$. The quantity $S^{\{A\}}$ is not submitted to the constraints imposed to S because entropy can be exchanged between the two subspaces. For instance, $S_{\rm VN}$ verifies the subadditivity and the Araki-Leib inequality

$$S^{\{AB\}}_{\rm VN} - S^{\{B\}}_{\rm VN} \leqslant S^{\{A\}}_{\rm VN} \leqslant S^{\{AB\}}_{\rm VN} + S^{\{B\}}_{\rm VN}, \tag{5}$$

where the maximum of $S^{\{B\}}_{\rm VN}$ is $\log M$ [23–26]. Using Eq. (2), we thus find the fundamental inequality

$$\frac{1}{M}D^{\{AB\}} \leqslant D^{\{A\}} \leqslant MD^{\{AB\}} \tag{6}$$

that bounds the PSD evolution. The gain limit of M is a fundamental result of our study. This latter also holds for $S^{\{A\}}_{\rm Sh}$ and consequently $D^{\{A\}}_{\rm Sh}$ can only increase by a factor M for an initial thermal state because $D^{\{A\}}_{\rm Sh} \leqslant D^{\{A\}}_{\rm VN}$ with both quantities being equal for an initial diagonal (or thermal) state. As discussed in Appendix C, this is general and can be extended to other PSD definitions based on entropy, functions, or maximum of PMD that are all bounded by the same factor M. This is consistent with our numerical results in Fig. 3 showing the evolution of the quantities max $[\hat{\rho}^A]$, max $[Q^{\{A\}}]$, $S^{\{A\}}_{\rm VN}$, and $S^{\{A\}}_{\rm Sh}$ [Eqs. (C2)–(C4)]. As an important precaution, we mention that using pseudo-phase-space-density definitions, as the ones filtering a specific state [such as for the ground state only $S^{(g)}_{\rm Sh}$; see Eq. (C4)], it is possible to find larger increase than a factor 2.

IV. CONCLUSION

In conclusion, in the absence of spontaneous emission and using classical laser fields, we have shown that a quantum description is more reliable than a semiclassical description of the atomic motion, which can lead to large errors. We have also shown that the total eigenvalues-based PSD cannot increase. This conclusion can be extended to informational population-based PSD (max $[\hat{\rho}]$, $S_{\rm Sh}$ entropy, or max $[Q]$) when the initial state is a diagonal state. Still, a sample initially prepared in a thermal state and thereby without quantum correlation can exhibit a gain of the PMD maximum or PSD up to the number M of internal states (or ultimately M^2 if initial correlations exist in the initial state; see Appendix C). The direct and fundamental consequence of this analysis, holding for any kind of free particles or particles in time-dependent trapping potential, is that cooling mechanisms based on coherent field momentum transfer without spontaneous emission (such as adiabatic passages, bichromatic, and π pulses [5,6,8,10,11,27]) have a limited efficiency and could only lead to a position-momentum PSD gain of M. This is still of interest for studies that need more particles in a same phase-space area regardless of the internal distribution (for laser manipulation, detection, collisional studies, etc.). However, increasing the full PSD is impossible; in other words, the production under coherent fields of all particles in the same internal state with a larger PSD than the initial one is impossible without spontaneous emission. An obvious way to overcome this limitation is to allow a single spontaneous emission event per particle [28–30] because the third ancilla spontaneous emission space has almost an infinite dimension to extract entropy (see [9,31–40]). A second option for cooling is to create entanglement between particles and the light field [41,42] or by using nonstatistical methods such as informational cooling (stochastic cooling being one famous example) [43,44] or cavity cooling [23,41,45–48]. A final alternative would be to use nonclassical quantum fields. Because absorption or stimulated emission rates are not equivalent anymore (with

the simple example of Fock states), the last step sketched in Fig. 1 would allow one to put more atoms at the same phase-space location [14]. In other words, when the optical field is no longer considered as a parameter, the total system is now composed of three subsystems (external, internal degrees of freedom, and quantized field). Our previous demonstrations could then be applied: the (external) PSD can be increased by the number of available microstates in the other (internal and field) spaces. If the latter are sufficiently large, there is *a priori* no theoretical limit on cooling even without spontaneous emission [3,7,9,10,23,45,47].

ACKNOWLEDGMENTS

The authors thank P. Cheinet for valuable advice. This work was supported by ANR MolSisCool, ANR HREELM, Dim Nano-K CPMV, CEFIPRA No. 5404-1, LabEx PALM ExciMol, and ATERSIIQ (No. ANR-10-LABX-0039-PALM).

T.C., D.C., and H.L. contributed equally to this work.

APPENDIX A: NONRELATIVISTIC HAMILTONIAN OF NONINTERACTING PARTICLES

We recall here the equations of motion for laser cooling of atoms. The reader can refer to textbooks such as [49].

1. Quantized or (semi)classical Hamiltonian

We study here the quantum Hamiltonian $\hat{H}$ of two generic levels $|1\rangle$ and $|2\rangle$ (representing the ground $|g\rangle$ and the excited $|e\rangle$ states in main text of a particle (mass m) under the effect of electromagnetic fields. The generalization to an M level system is straightforward but will not be detailed for the sake of simplicity. We separate the "motional" (or trapping) fields that do not couple $|1\rangle$ and $|2\rangle$, such as trapping potential V_1, V_2 produced for example by magnetic coils, magnets, or electrodes through Zeeman ($-\hat{\boldsymbol{\mu}}.\boldsymbol{B}$) or Stark effect ($-\hat{\boldsymbol{d}}.\boldsymbol{E}$), and the laser fields $\hat{\boldsymbol{E}}$ that do couple $|1\rangle$ and $|2\rangle$.

For N noninteracting particles the full Hamiltonian can be written as $\hat{H} = \sum_{i=1}^{N} \hat{H}^{(i)} + \hat{H}_{\text{field}} + \sum_{i=1}^{N} \hat{H}^{(i)}_{\text{int,field}}$, where $\hat{H}^{(i)}$ is the Hamiltonian $\frac{\hat{p}_i^2}{2m} + V_1(\hat{\boldsymbol{r}}_i, t)|1\rangle\langle 1| + V_2(\hat{\boldsymbol{r}}_i, t)|2\rangle\langle 2|$ for the position and momentum $\boldsymbol{p}_i, \boldsymbol{r}_i$ of the ith particle. The trapping field is arbitrary but the simplest case corresponds to harmonic traps: $V_i = E_i + \frac{1}{2}m\omega_i \boldsymbol{r}^2$. A base of the Hilbert space will be an ensemble of states $\bigotimes_{i=1}^{N} |\boldsymbol{p}_i, 1 \text{ or } 2\rangle_i \otimes |\pi_{\boldsymbol{k}\sigma} n_{\boldsymbol{k}\sigma}\rangle$ when using the Fock notation for the field. We treat the N particles as totally independent and use the density-matrix formalism (written as $\hat{\rho}$) to describe the system of N identical particles as a statistical ensemble. The external field is common to the N atoms and this can automatically generate entanglement between the atoms or collective behavior that can indeed lead to cooling [41,42]. As explained in the article, this is not our interest here and we shall study only the single-particle case. In the dipolar approximation and neglecting the Roentgen term, despite the fact that it can create surprising radiation forces on the atoms [50,51], the Hamiltonian for a single particle reads as

$$\hat{H} = \frac{\hat{\boldsymbol{p}}^2}{2m} + V_1(\hat{\boldsymbol{r}}, t)|1\rangle\langle 1| + V_2(\hat{\boldsymbol{r}}, t)|2\rangle\langle 2| - \boldsymbol{d} \cdot \hat{\boldsymbol{E}}(\hat{\boldsymbol{r}}, t) \times (|2\rangle\langle 1| + |1\rangle\langle 2|) + \sum_{\boldsymbol{k}\sigma} \hbar\omega_k (\hat{a}^{\dagger}_{\boldsymbol{k}\sigma}\hat{a}_{\boldsymbol{k}\sigma} + 1/2), \quad \text{(A1)}$$

where $\boldsymbol{d}$ is the transition dipole element (assumed to be real $\boldsymbol{d} = \langle 2|q\hat{\boldsymbol{r}}|1\rangle$) and $\hat{\boldsymbol{E}}(\boldsymbol{r}, t)$ is a quantized real field. For instance for a single plane wave field (in a volume L^3) $\hat{\boldsymbol{E}}(\boldsymbol{r}, t) = \sum_{\boldsymbol{k},\sigma} i\sqrt{\frac{\hbar\omega_k}{2\epsilon_0 L^3}}(\hat{a}_{\boldsymbol{k}\sigma} e^{-i\omega_k t}\boldsymbol{\epsilon}_{\boldsymbol{k}\sigma} \mathrm{e}^{i\boldsymbol{k}.\boldsymbol{r}} - \hat{a}^{\dagger}_{\boldsymbol{k}\sigma} e^{i\omega_k t}\boldsymbol{\epsilon}^{*}_{\boldsymbol{k}\sigma} \mathrm{e}^{-i\boldsymbol{k}.\boldsymbol{r}})$.

The initial state is uncorrelated and the density operator can be written as an atomic (external and internal degrees of freedom) and a field part as $\hat{\rho} = \hat{\rho}_{\text{at}} \otimes \hat{\rho}_{\text{field}} = \hat{\rho}_{\text{ext}} \otimes \hat{\rho}_{\text{int}} \otimes \hat{\rho}_{\text{field}}$.

In the semiclassical approximation, we would like to replace the field operators (denoted with the hat $\hat{}$) by their classical expectation values, namely $\hat{a}_{\boldsymbol{k}\sigma}$ and $\hat{a}^{\dagger}_{\boldsymbol{k}\sigma}$ by c numbers $a_{\boldsymbol{k}\sigma}$ and $a^{*}_{\boldsymbol{k}\sigma}$, such as $\hat{\boldsymbol{E}}(\hat{\boldsymbol{r}}, t)$ by $\boldsymbol{E}(\hat{\boldsymbol{r}}, t)$ becomes in the Hamiltonian

$$\hat{H} = \frac{\hat{\boldsymbol{p}}^2}{2m} + E_1(\hat{\boldsymbol{r}}, t)|1\rangle\langle 1| + E_2(\hat{\boldsymbol{r}}, t)|2\rangle\langle 2| - \boldsymbol{d} \cdot \boldsymbol{E}(\hat{\boldsymbol{r}}, t)(|2\rangle\langle 1| + |1\rangle\langle 2|).$$

2. Classical fields

This can be done by using coherent states $|\alpha\rangle$, that are eigenstates of the annihilation operator $\hat{a}$: $\hat{a}|\alpha\rangle = \alpha|\alpha\rangle$, by using the unitary transformation under the operator $\hat{U} = \hat{\mathcal{D}}(\alpha_\lambda e^{-i\omega_\lambda})^{\dagger}$, and neglecting the quantum field that now describes spontaneous emission only [12–14].

Therefore, in the following we assume to have classical laser fields with different frequencies ω_{L}, wave vectors $\boldsymbol{k}_{\text{L}}$, or temporal phase $\Phi_{\text{L}}(t)$: $\boldsymbol{E}(\hat{\boldsymbol{r}}, t) = \boldsymbol{E}'(\hat{\boldsymbol{r}}, t) + \boldsymbol{E}'^{\dagger}(\hat{\boldsymbol{r}}, t) = \frac{1}{2}\sum_{\text{L}} [\boldsymbol{E}_{\text{L}}(t)e^{i[\boldsymbol{k}_{\text{L}}\cdot\hat{\boldsymbol{r}} - \omega_{\text{L}}t - \Phi_{\text{L}}(t)]} + \boldsymbol{E}^{*}_{\text{L}}(t)e^{-i[\boldsymbol{k}_{\text{L}}\cdot\hat{\boldsymbol{r}} - \omega_{\text{L}}t - \Phi_{\text{L}}(t)]}]$. The rotating wave approximation leads to

$$\hat{H} = \frac{\hat{\boldsymbol{p}}^2}{2m} + V_1(\hat{\boldsymbol{r}}, t)|1\rangle\langle 1| + V_2(\hat{\boldsymbol{r}}, t)|2\rangle\langle 2| - \boldsymbol{d} \cdot \boldsymbol{E}'(\hat{\boldsymbol{r}}, t)|2\rangle\langle 1| - \boldsymbol{d} \cdot \boldsymbol{E}'^{\dagger}(\hat{\boldsymbol{r}}, t)|1\rangle\langle 2|). \quad \text{(A2)}$$

We will now use this Hamiltonian to describe the evolution. In matrix notation with the $|1, 2\rangle$ basis, the Hamiltonian (A2) becomes $\hat{H} = \begin{pmatrix} \hat{H}_1 & \hat{V}^{\dagger} \\ \hat{V} & \hat{H}_2 \end{pmatrix}$, where the coupling term is $\hat{V} = -\boldsymbol{d} \cdot \boldsymbol{E}'(\hat{r}, t) = -\frac{d}{2}\sum_{\text{L}} \boldsymbol{E}_{\text{L}}(t)e^{i[\boldsymbol{k}_{\text{L}}\cdot\hat{\boldsymbol{r}} - \omega_{\text{L}}t - \Phi_{\text{L}}(t)]} = \sum_{\text{L}} \hat{V}_{\text{L}}$.

a. Density matrix

The time evolution $i\hbar\frac{\partial\hat{\rho}}{\partial t} = \hat{H}\hat{\rho} - \hat{\rho}\hat{H}$ leads to

$$\begin{pmatrix} \frac{\partial\hat{\rho}_{11}}{\partial t} & \frac{\partial\hat{\rho}_{12}}{\partial t} \\ \frac{\partial\hat{\rho}_{21}}{\partial t} & \frac{\partial\hat{\rho}_{22}}{\partial t} \end{pmatrix} = \frac{1}{i\hbar}\begin{pmatrix} [\hat{H}_1, \hat{\rho}_{11}] + \hat{V}^\dagger\hat{\rho}_{21} - \hat{\rho}_{12}\hat{V} & [\hat{p}^2/2m, \hat{\rho}_{12}] + \hat{V}_1\hat{\rho}_{12} - \hat{\rho}_{12}\hat{V}_2 + \hat{V}^\dagger\hat{\rho}_{22} - \hat{\rho}_{11}\hat{V}^\dagger \\ [\hat{p}^2/2m, \hat{\rho}_{21}] + \hat{V}_2\hat{\rho}_{21} - \hat{\rho}_{21}\hat{V}_1 + \hat{V}\hat{\rho}_{11} - \hat{\rho}_{22}\hat{V} & [\hat{H}_2, \hat{\rho}_{22}] + \hat{V}\hat{\rho}_{12} - \hat{\rho}_{21}\hat{V}^\dagger \end{pmatrix}.$$

b. Wigner functions

The Wigner-Weyl transform of this equation gives the time evolution of the Wigner function defined as

$$W(\boldsymbol{r}, \boldsymbol{p}, t) = \frac{1}{h^3}\int \langle \boldsymbol{p} - \boldsymbol{p}'/2|\hat{\rho}(\hat{\boldsymbol{r}}, \hat{\boldsymbol{p}}, t)|\boldsymbol{p} + \boldsymbol{p}'/2\rangle e^{-i\boldsymbol{r}\cdot\boldsymbol{p}'/\hbar} d\boldsymbol{p}' \tag{A3}$$

through the so-called Moyal bracket, governed by

$$\frac{\partial W}{\partial t} = \frac{1}{i\hbar}(H \star W - W \star H). \tag{A4}$$

The $\star$ product can be evaluated using the convenient formula [21] for any generic function $\rho_{1,2}(r, p)$,

$$(\rho_1 \star \rho_2)(r, p) = \rho_1\left(r + i\frac{\hbar}{2}\frac{\partial}{\partial p}, p - i\frac{\hbar}{2}\frac{\partial}{\partial r}\right)\rho_2(r, p),$$
$$(\rho_2 \star \rho_1)(r, p) = \rho_2\left(r - i\frac{\hbar}{2}\frac{\partial}{\partial p}, p + i\frac{\hbar}{2}\frac{\partial}{\partial r}\right)\rho_1(r, p),$$

that we have restricted to a one-dimensional motion for simplicity.

Therefore, when no $\hat{r}$, $\hat{p}$ product is present in $\hat{\rho} = \rho(\hat{r}, \hat{p})$, the Wigner-Weyl transform $W_{\hat{\rho}}(r, p; t)$ is the unmodified classical observable expression $\rho(r, p)$. An important example is a conventional Hamiltonian, $\hat{H} = \hat{p}^2/2m + V(\hat{r}, t)$, for which the transition from classical mechanics is the straightforward quantization: $W_{\hat{H}}(r, p; t) = H(r, p; t) = p^2/2m + V(r, t)$.

The expressions containing $e^{i\boldsymbol{k}_L\cdot\hat{\boldsymbol{r}}}$ can be expanded by using an exponential (Taylor) series that indicates $e^{ik_L(r\pm\frac{i\hbar}{2}\frac{\partial}{\partial p})}f(r, p, t) = e^{ik_L r}f(r, p \mp \hbar k_L/2, t)$. and finally using $\hbar\omega_L(r, t) = \boldsymbol{d}\cdot\boldsymbol{E}_L e^{i[k_L\cdot\boldsymbol{r} - \omega_L t - \Phi_L(t)]}$, we obtain

$$\left\{\frac{\partial}{\partial t} + \frac{p}{m}\frac{\partial}{\partial r} - \frac{1}{i\hbar}\left[V_1\left(r + i\frac{\hbar}{2}\partial_p\right) - V_1\left(r - i\frac{\hbar}{2}\partial_p\right)\right]\right\}W_{11}(r, p, t)$$
$$= -\frac{1}{2i}\sum_L\left[\Omega_L^*(r, t)W_{21}\left(r, p + \frac{\hbar k_L}{2}, t\right) - \Omega_L(r, t)W_{12}\left(r, p + \frac{\hbar k_L}{2}, t\right)\right], \tag{A5}$$

$$\left\{\frac{\partial}{\partial t} + \frac{p}{m}\frac{\partial}{\partial r} - \frac{1}{i\hbar}\left[V_1\left(r + i\frac{\hbar}{2}\partial_p\right) - V_2\left(r - i\frac{\hbar}{2}\partial_p\right)\right]\right\}W_{12}(r, p, t)$$
$$= -\frac{1}{2i}\sum_L\Omega_L^*(r, t)\left[W_{22}\left(r, p + \frac{\hbar k_L}{2}, t\right) - W_{11}\left(r, p - \frac{\hbar k_L}{2}, t\right)\right], \tag{A6}$$

$$\left\{\frac{\partial}{\partial t} + \frac{p}{m}\frac{\partial}{\partial r} - \frac{1}{i\hbar}\left[V_2\left(r + i\frac{\hbar}{2}\partial_p\right) - V_1\left(r - i\frac{\hbar}{2}\partial_p\right)\right]\right\}W_{21}(r, p, t)$$
$$= -\frac{1}{2i}\sum_L\Omega_L(r, t)\left[W_{11}\left(r, p - \frac{\hbar k_L}{2}, t\right) - W_{22}\left(r, p + \frac{\hbar k_L}{2}, t\right)\right], \tag{A7}$$

$$\left\{\frac{\partial}{\partial t} + \frac{p}{m}\frac{\partial}{\partial r} - \frac{1}{i\hbar}\left[V_2\left(r + i\frac{\hbar}{2}\partial_p\right) - V_2\left(r - i\frac{\hbar}{2}\partial_p\right)\right]\right\}W_{22}(r, p, t)$$
$$= -\frac{1}{2i}\sum_L\left[\Omega_L(r, t)W_{12}\left(r, p - \frac{\hbar k_L}{2}, t\right) - \Omega_L^*(r, t)W_{21}\left(r, p - \frac{\hbar k_L}{2}, t\right)\right]. \tag{A8}$$

For completeness, we mention that a (1D) spontaneous emission rate Γ can be added if needed, by including the terms [20,52]

$$\left.\frac{\partial W_{11}}{\partial t}\right|_{\text{spon}} = \Gamma\int_{-p_r}^{p_r}\Theta(p')W_{22}(r, p + p')dp', \quad \left.\frac{\partial W_{11}}{\partial t}\right|_{\text{spon}} = -\frac{\Gamma}{2}W_{12}(r, p),$$
$$\left.\frac{\partial W_{21}}{\partial t}\right|_{\text{spon}} = -\frac{\Gamma}{2}W_{21}(r, p), \quad \left.\frac{\partial W_{22}}{\partial t}\right|_{\text{spon}} = -\Gamma W_{22}(r, p),$$

where $\Theta(p')$ is the probability density distribution for the projection of spontaneous emission $\Theta(p') = \frac{3}{8p_r}(1 + \frac{p'^2}{p_r^2})$ (for a dipolar radiation pattern) on the atomic recoil momentum for $p_r = \hbar k$. Equation of motion of the Husimi distribution can be derived [53–57] and presents a nonzero second term of the Liouville equation [similar to Eqs. (A5)–(A8)].

3. Connection with Liouville equation

In the absence of light fields, Taylor series expansion indicates that the evolution of the diagonal terms W_{ii} is given by

$$\frac{DW_{ii}}{Dt} = \frac{\partial W_{ii}}{\partial t} + \frac{p}{m}\cdot\frac{\partial W_{ii}}{\partial r} - \frac{\partial V_i}{\partial r}\cdot\frac{\partial W_{ii}}{\partial p} = \sum_{s\geqslant 1}\hbar^{2s}\frac{2^{-2s}}{(2s+1)!}\frac{\partial^{2s+1}V_i}{\partial r^{2s+1}}\frac{\partial^{2s+1}W_{ii}}{\partial p^{2s+1}}.$$

We recover the Liouville's equation, $\frac{DW_{ii}}{Dt} = 0$, under the influence of the potential V, but only for a quadratic potential $V_i(r,t) = a(t) + b(t)r + c(t)r^2$. However, when higher derivatives of $V_i(r)$ are present, additional terms will give rise to diffusion and the quantum Wigner function gradually deviates from the corresponding classical phase-space probability density. So a nonharmonic potential is a clear way to modify the Wigner phase-space density. This argument also applies to the Husimi function.

4. Interaction picture: Free evolution

The evolution of $H_1(t)$ is given by the unitary time evolution operator $\hat{U}_1(t) = e^{-i\int \hat{H}_1(t)/\hbar}$. In matrix notation, the evolution operator is $\hat{U}_0 = \begin{pmatrix}\hat{U}_1 & 0\\ 0 & \hat{U}_2\end{pmatrix}$. The interaction picture consists in defining a new density matrix $\hat{\rho}^I(t) = \hat{U}_0^\dagger(t)\hat{\rho}(t)\hat{U}_0(t)$, which evolves under the modified Hamiltonian $\hat{H}^I = \hat{U}_0^\dagger\hat{H}\hat{U}_0 + i\hbar\frac{d\hat{U}_0^\dagger}{dt}\hat{U}_0 = \begin{pmatrix}0 & \hat{V}^{I\dagger}\\ \hat{V}^I & 0\end{pmatrix}$, where $\hat{V}^I = \hat{U}_2^\dagger\hat{V}\hat{U}_1$.

Because several laser frequencies are possibly present, the interaction picture is more appropriate than the Bloch rotating frame. The latter would imply to choose one laser frequency as a reference. The interaction picture removes this arbitrariness.

a. Density matrix

Using the momentum representation, where $\hat{r}$ acts as $i\hbar\partial_p$ on $\psi(p) = \langle p|\psi\rangle$, we have $e^{ik\hat{r}}|p\rangle = |p + \hbar k\rangle$. We find

$$\hat{V}^I|p\rangle = -\frac{1}{2}\sum_{\rm L}|p + \hbar k_L\rangle\Omega_{\rm L}e^{-i(\delta_{\rm L}^{p+}t)}, \tag{A9}$$

$$\delta_{\rm L}^{p\pm} = \omega_{\rm L} - (E_2 - E_1)/\hbar - \frac{k_{\rm L}}{m}(p \pm \hbar k_{\rm L}/2), \tag{A10}$$

where $\hbar\Omega_{\rm L}(t) = \boldsymbol{d}\cdot\boldsymbol{E}_{\rm L}e^{-\Phi_{\rm L}(t)}$ and $\delta_{\rm L}^{p\pm} = \delta_{\rm L}^0 + \delta_{\rm L}^{\rm D}(p) \pm \delta_{\rm L}^{\rm r}$: the detuning $\delta_{\rm L}^0 = \omega_{\rm L} - (E_2 - E_1)/\hbar$, the Doppler shift $\delta_{\rm L}^{\rm D}(p) = -k_{\rm L}.p/m$, and recoil frequency $\delta_{\rm L}^{\rm r} = -\hbar k_{\rm L}^2/2m$ appear naturally.

With $\hat{\rho}_{ij}^I = \hat{U}_i^\dagger\hat{\rho}_{ij}\hat{U}_j$, the evolution reads as

$$\begin{pmatrix}\frac{\partial\hat{\rho}_{11}^I}{\partial t} & \frac{\partial\hat{\rho}_{12}^I}{\partial t}\\ \frac{\partial\hat{\rho}_{21}^I}{\partial t} & \frac{\partial\hat{\rho}_{22}^I}{\partial t}\end{pmatrix} = \frac{1}{i\hbar}\sum_{\rm L}\begin{pmatrix}\hat{V}^{I\dagger}\hat{\rho}_{21}^I - \hat{\rho}_{12}^I\hat{V}^I & \hat{V}^{I\dagger}\hat{\rho}_{22}^I - \hat{\rho}_{11}^I\hat{V}^{I\dagger}\\ \hat{V}^I\hat{\rho}_{11}^I - \hat{\rho}_{22}^I\hat{V}^I & \hat{V}^I\hat{\rho}_{12}^I - \hat{\rho}_{21}^I\hat{V}^{I\dagger}\end{pmatrix}. \tag{A11}$$

Assuming there is no external field from now on and using ${\rho^I}_{ij}^{p'p} = \langle p'|\hat{\rho}_{ij}^I|p\rangle = e^{i(p'^2-p^2)t/2m\hbar}e^{i(E_i-E_j)t/\hbar}\rho_{ij}^{p'p}$, the latter can be written as

$$\begin{pmatrix}\frac{\partial{\rho^I}_{11}^{p'p}}{\partial t} & \frac{\partial{\rho^I}_{12}^{p'p}}{\partial t}\\ \frac{\partial{\rho^I}_{21}^{p'p}}{\partial t} & \frac{\partial{\rho^I}_{22}^{p'p}}{\partial t}\end{pmatrix} = -\frac{1}{2i}\sum_{\rm L}\begin{pmatrix}\Omega_{\rm L}^*e^{i\delta_{\rm L}^{p'+}t}{\rho^I}_{21}^{(p'+\hbar k_{\rm L})p} - \Omega_{\rm L}{\rho^I}_{12}^{p'(p+\hbar k_{\rm L})}e^{-i\delta_{\rm L}^{p+}t} & \Omega_{\rm L}^*e^{i\delta_{\rm L}^{p'+}t}{\rho^I}_{22}^{(p'+\hbar k_{\rm L})p} - \Omega_{\rm L}^*{\rho^I}_{11}^{p'(p-\hbar k_{\rm L})}e^{i\delta_{\rm L}^{p-}t}\\ \Omega_{\rm L}e^{-i\delta_{\rm L}^{p'-}t}{\rho^I}_{11}^{(p'-\hbar k_{\rm L})p} - \Omega_{\rm L}{\rho^I}_{22}^{p'(p+\hbar k_{\rm L})}e^{-i\delta_{\rm L}^{p+}t} & \Omega_{\rm L}e^{-i\delta_{\rm L}^{p'-}t}{\rho^I}_{12}^{(p'-\hbar k_{\rm L})p} - \Omega_{\rm L}^*{\rho^I}_{21}^{p'(p-\hbar k_{\rm L})}e^{i\delta_{\rm L}^{p-}t}\end{pmatrix}. \tag{A12}$$

b. Wigner function

It is quite convenient to use the so-called nondiagonal Wigner functions by defining $W_{ij}^I = W_{\hat{\rho}_{ij}^I}/h$ as the Wigner transform function associated to $\hat{\rho}_{ij}^I = \langle i|\hat{\rho}^I|j\rangle$. So $W_{ij}(r,p,t) = e^{i(E_j-E_i)t/\hbar}W_{ij}^I(r - pt/m, p, t)$ and the evolution equations become

$$\frac{\partial W_{11}^I}{\partial t}(r,p,t) = -\sum_{\rm L}{\rm Im}\big[\Omega_L^*(r,p,t)W_{21}^I(r - \hbar k_{\rm L}t/2m, p + \hbar k_{\rm L}/2, t)\big], \tag{A13}$$

$$\frac{\partial W_{21}^I}{\partial t}(r,p,t) = \frac{1}{2i}\sum_{\rm L}\Omega_L(r,p,t)\big[W_{22}^I(r - \hbar k_{\rm L}t/2m, p + \hbar k_{\rm L}/2, t) - W_{11}^I(r + \hbar k_{\rm L}t/2m, p - \hbar k_{\rm L}/2, t)\big], \tag{A14}$$

$$\frac{\partial W_{22}^I}{\partial t}(r,p,t) = \sum_{\rm L}{\rm Im}\big[\Omega_L^*(r,p,t)W_{21}^I(r + \hbar k_{\rm L}t/2m, p - \hbar k_{\rm L}/2, t)\big], \tag{A15}$$

where

$$\Omega_{\mathrm{L}}(r,\,p,\,t)=\Omega_{\mathrm{L}}e^{i[k_{L}r+k_{\mathrm{L}}pt/m-\delta_{\mathrm{L}}^{0}t-\Phi_{\mathrm{L}}(t)]}. \tag{A16}$$

5. Single laser case (Bloch equation)

When there is only one laser, we can define

$$\tilde{W}_{11}^{I}(r,\,p,\,t)=W_{11}^{I}(r,\,p,\,t),\quad \tilde{W}_{22}^{I}(r,\,p,\,t)=W_{22}^{I}(r-\hbar k_{\mathrm{L}}t/m,\,p+\hbar k_{\mathrm{L}},\,t),$$
$$\tilde{W}_{21}^{I}(r,\,p,\,t)=e^{-i(k_{\mathrm{L}}r+\frac{k_{\mathrm{L}}pt}{m}-\delta_{\mathrm{L}}^{0}t-\Phi_{\mathrm{L}})}W_{21}^{I}\left(r-\frac{\hbar k_{\mathrm{L}}t}{2m},\,p+\frac{\hbar k_{\mathrm{L}}}{2},\,t\right).$$

If we assume Ω_{L} real, the evolution is governed by

$$\frac{\partial}{\partial t}\frac{\tilde{W}_{11}^{I}-\tilde{W}_{22}^{I}}{2}=-\Omega_{L}\mathrm{Im}\tilde{W}_{21}^{I}+\frac{\hbar k_{\mathrm{L}}}{2m}\frac{\partial}{\partial r}\tilde{W}_{22}^{I}, \tag{A17}$$

$$\frac{\partial}{\partial t}\mathrm{Re}\tilde{W}_{21}^{I}=-\delta_{\mathrm{L}}^{p+}\mathrm{Im}\tilde{W}_{21}^{I}-\frac{\hbar k_{\mathrm{L}}}{2m}\frac{\partial}{\partial r}\mathrm{Re}\tilde{W}_{21}^{I}, \tag{A18}$$

$$\frac{\partial}{\partial t}\mathrm{Im}\tilde{W}_{21}^{I}=\delta_{\mathrm{L}}^{p+}\mathrm{Re}\tilde{W}_{21}^{I}+\Omega_{L}\frac{\tilde{W}_{11}^{I}-\tilde{W}_{22}^{I}}{2}-\frac{\hbar k_{\mathrm{L}}}{2m}\frac{\partial}{\partial r}\mathrm{Im}\tilde{W}_{21}^{I}. \tag{A19}$$

We recognize the standard Bloch equations except for the term in $\frac{\hbar k_{\mathrm{L}}}{2m}\frac{\partial}{\partial r}$. We can thus retrieve the Bloch equations from the exact Wigner function evolution by performing series expansion in $\hbar k$. This approach justifies the semiclassical equation for the particle's evolution that we derive from heuristic considerations.

APPENDIX B: SEMICLASSICAL EVOLUTION

From the quantum evolution, we can derive the semiclassical evolution of the atomic motion. The underlying assumption is that the displacement of the atom during the internal relaxation time is very small. The internal variables follow quasiadiabatically the external motion [20]. It is then possible to separate the internal and the external degree of freedom.

The Doppler or recoil effects, or the use of the stationary state of the Bloch equation, can be done with hand-waving arguments (see for instance [58]). Nevertheless, the Lagrangian description (individual particles are followed through time), Eulerian description, and interaction picture that freeze the motion in the Eulerian description may lead to confusion. We will clarify this distinction.

1. Definition of the force

For simplicity, we neglect the external potentials (but they can be included in the interaction picture if needed).

In the semiclassical approach, the particle motion is classical: for a given particle initially at $\boldsymbol{r}(t_0)=\boldsymbol{r}_0$ and $\boldsymbol{v}(t_0)=\boldsymbol{v}_0$ at time $t=t_0$ its trajectory in phase space $\boldsymbol{r}(t)$, $\boldsymbol{p}(t)=m\boldsymbol{v}(t)$ is given by Newton's equation of motion $m\frac{d\boldsymbol{v}}{dt}(t)=\boldsymbol{F}(\boldsymbol{r}(t),\boldsymbol{v}(t),t)$.

The standard way to define the force in laser cooling is by using the Ehrenfest theorem (see for instance [59,60], but other methods exist [61–63]). Knowing the light field seen by the atom at the position $\boldsymbol{r}$ with velocity $\boldsymbol{v}=\boldsymbol{p}/m$ enables one to solve the optical Bloch equations [density matrix $\hat{\sigma}(t)$ evolution] to determine the atomic internal state. The force is then derived from $\boldsymbol{F}=-\mathrm{tr}[\hat{\sigma}(t)\nabla\hat{H}]=\langle\frac{\partial\boldsymbol{d}\cdot\boldsymbol{E}}{\partial\boldsymbol{r}}\rangle$. The usual optical Bloch equations where $\sigma_{ij}(t)$ stands for $\sigma_{ij}(t;r_0,\,v_0,\,t_0)$ read as

$$\begin{pmatrix}\frac{\partial\sigma_{11}}{\partial t} & \frac{\partial\sigma_{12}}{\partial t}\\ \frac{\partial\sigma_{21}}{\partial t} & \frac{\partial\sigma_{22}}{\partial t}\end{pmatrix}(t)=-\frac{1}{2i}\sum_{\mathrm{L}}\begin{pmatrix}\Omega_{\mathrm{L}}^{*}(r(t),t)\sigma_{21}(t)-\Omega_{\mathrm{L}}(r(t),t)\sigma_{12}(t) & \Omega_{\mathrm{L}}^{*}(r(t),t)[\sigma_{22}(t)-\sigma_{11}(t)]\\ \Omega_{\mathrm{L}}(r(t),t)[\sigma_{11}(t)-\sigma_{22}(t)] & \Omega_{\mathrm{L}}(r(t),t)\sigma_{12}(t)-\Omega_{\mathrm{L}}^{*}(r(t),t)\sigma_{21}(t)\end{pmatrix}, \tag{B1}$$

where $\Omega_{\mathrm{L}}(r,t)=\Omega_{\mathrm{L}}e^{i(\boldsymbol{k}_{\mathrm{L}}.\boldsymbol{r}-\Omega_{\mathrm{L}}t-\Phi_{\mathrm{L}})}$. The rapidly oscillating terms can be removed by introducing slowly varying quantities as $\sigma_{ij}^{I}(t)=e^{-i(E_j-E_i)t/\hbar}\sigma_{ij}(t)$.

The absence of Doppler shift in the expression of $\Omega_{\mathrm{L}}(r,t)$ may be surprising, especially when compared to Eq. (A12) [using $p'=p=p(t)$, $r=r(t)$, and $\hbar k_{\mathrm{L}}$ put to zero]. The explanation is the following: we use $\boldsymbol{r}(t)=\boldsymbol{r}(t;\boldsymbol{r}_0,\boldsymbol{v}_0,t_0)$, the Lagrangian description where individual particles are followed through time, whereas, when dealing with the Wigner $W(\boldsymbol{r},\boldsymbol{v},t)$ or position-momentum distribution $\rho(\boldsymbol{r},\boldsymbol{v},t)$ picture, we use the Eulerian description. The connection between Lagrangian and Eulerian coordinates explains why the Doppler effect is correctly taken in both Eq. (B1) with $\Omega_{\mathrm{L}}(r(t),t)=\Omega_{\mathrm{L}}e^{i[\boldsymbol{k}_{\mathrm{L}}.\boldsymbol{r}(t)-\Omega_{\mathrm{L}}t-\Phi_{\mathrm{L}}(t)]}$ and in Eq. (A12) with $\Omega_{\mathrm{L}}(r,\,p,\,t)=\Omega_{\mathrm{L}}e^{i[k_{L}r+k_{\mathrm{L}}pt/m-\delta_{\mathrm{L}}^{0}t-\Phi_{\mathrm{L}}(t)]}$. In any case, the instantaneous laser phase seen by the atoms is correct, including the Doppler effect because $\frac{dr(t)}{dt}=p(t)/m$.

Similarly, in the Eulerian description the force is thus given by $\mathrm{Tr}[\hat{\sigma}(t)\nabla\hat{H}]$ or $\mathrm{Tr}[\hat{\rho}(t)^{I}\nabla\hat{V}^{I}]$ using the cyclic invariant of the trace. We have $V^{I}(r,\,p,\,t)=-\sum_{\mathrm{L}}\frac{\hbar}{2}\Omega_{\mathrm{L}}(r,\,p,\,t)$ so $\nabla V^{I}(r,\,p,\,t)=-i\sum_{\mathrm{L}}\frac{\hbar\boldsymbol{k}_{\mathrm{L}}}{2}\Omega_{\mathrm{L}}(r,\,p,\,t)$.

So in conclusion and back to our Lagrangian description we have

$$\boldsymbol{F}(\boldsymbol{r}(t),\boldsymbol{v}(t),t)=\mathrm{Im}\left[\sigma_{21}(t)\sum_{\mathrm{L}}\hbar\boldsymbol{k}_{\mathrm{L}}\Omega_{\mathrm{L}}^{*}(\boldsymbol{r}(t),t)\right]. \tag{B2}$$

As we chose plane waves (or $\nabla E_{\mathrm{L}}=0$), there is no direct dipolar force. Also, because of the interplay between the Bloch equations [Eq. (B1)] and the force [Eq. (B2)], the atomic velocity $\boldsymbol{v}(t)$ and position $\boldsymbol{r}(t)$ should be updated in a short time interval (typically ps), and the calculation of the Bloch equation evolution iterated on a similar time scale [58].

2. Phase-space evolution equation

Here, we would like to justify the equations we just derived assuming a separation of the external and internal degrees of freedom. However, we know that, without spontaneous emission, this is valid only if the ratio of resonant photon momentum to atomic momentum dispersion is small $\hbar k/\Delta p\ll 1$. In such a case, the rapid processes acting on the internal degrees of freedom can be separated from the slow processes associated with translational motion. The dynamics of the atomic ensemble is thus determined by the slow change of the distribution function in translational degrees of freedom $w(r,p)=W_{11}+W_{22}$ and the expansion in $\hbar k$, that we will derive here for completeness, is justified [20].

One analog of the classical phase-space distribution ρ is the total distribution function in translational degrees of freedom, $w(r,p,t)$, as plotted in Fig. 2(b). Equations (A5)–(A8) (written for simplicity without the external potentials), become

$$\left[\frac{\partial}{\partial t}+\frac{p}{m}\frac{\partial}{\partial r}\right]W_{11}(r,p,t)=-\frac{1}{2i}\sum_{\mathrm{L}}[\Omega_{L}^{*}(r,t)W_{21}(r,p+\hbar k_{\mathrm{L}}/2,t)-\Omega_{L}(r,t)W_{12}(r,p+\hbar k_{\mathrm{L}}/2,t)]. \tag{B3}$$

$$\left[\frac{\partial}{\partial t}+\frac{p}{m}\frac{\partial}{\partial r}-\frac{E_1-E_2}{i\hbar}\right]W_{12}(r,p,t)=-\frac{1}{2i}\sum_{\mathrm{L}}\Omega_{L}^{*}(r,t)[W_{22}(r,p+\hbar k_{\mathrm{L}}/2,t)-W_{11}(r,p-\hbar k_{\mathrm{L}}/2,t)], \tag{B4}$$

$$\left[\frac{\partial}{\partial t}+\frac{p}{m}\frac{\partial}{\partial r}+\frac{E_1-E_2}{i\hbar}\right]W_{21}(r,p,t)=-\frac{1}{2i}\sum_{\mathrm{L}}\Omega_{L}(r,t)[W_{11}(r,p-\hbar k_{\mathrm{L}}/2,t)-W_{22}(r,p+\hbar k_{\mathrm{L}}/2,t)], \tag{B5}$$

$$\left[\frac{\partial}{\partial t}+\frac{p}{m}\frac{\partial}{\partial r}\right]W_{22}(r,p,t)=-\frac{1}{2i}\sum_{\mathrm{L}}[\Omega_{L}(r,t)W_{12}(r,p-\hbar k_{\mathrm{L}}/2,t)-\Omega_{L}^{*}(r,t)W_{21}(r,p-\hbar k_{\mathrm{L}}/2,t)], \tag{B6}$$

with $\hbar\Omega_{\mathrm{L}}(r,t)=\boldsymbol{d}\cdot\boldsymbol{E}_{\mathrm{L}}e^{i(k_{\mathrm{L}}\cdot r-\Omega_{\mathrm{L}}t-\Phi_{\mathrm{L}})}$.

A frequently used method to derive a continuity equation such as Eq. (1) for $\rho=w$ is to expand the Wigner distribution equations in a power series of the photon momentum $\hbar k$ [20,52,64–68]. In the presence of spontaneous emission, the second order leads to the standard Fokker-Planck equation [20,52,64–68]. The simplest formulation is restricted to the first-order approximation; therefore, $W_{21}(r,p\mp\hbar k_{\mathrm{L}}/2,t)\approx W_{21}(r,p,t)\mp\frac{\hbar k_{\mathrm{L}}}{2}\frac{\partial}{\partial p}\tilde{W}_{21}(r,p,t)$. To this first order in $\hbar k_{\mathrm{L}}$, the sum of (B3) and (B6) is

$$\left[\frac{\partial}{\partial t}+\frac{p}{m}\frac{\partial}{\partial r}\right]w(r,p,t)=-\sum_{\mathrm{L}}\mathrm{Im}\left[\Omega_{L}^{*}(r,t)\hbar k_{\mathrm{L}}\frac{\partial}{\partial p}W_{21}(r,p,t)\right]. \tag{B7}$$

Since the recoil momentum $\hbar k$ is small, the variation of atomic translational motion is slower than the atomic internal state change. The latter follows the varying translational state $w(r,p,t)$ [69]. Fast relaxation of the internal atomic state means that the functions $W_{ij}(r,p,t)$ follow the distribution function $w(r,p,t)$.

At zero order in $\hbar k_{\mathrm{L}}$ we have the simplest approximation $W_{ij}(r,p,t)\approx W_{ij}^{0}(r,p,t)w(r,p,t)$. Equation (B7) leads to

$$\left[\frac{\partial}{\partial t}+\frac{p}{m}\frac{\partial}{\partial r}\right]w(r,p,t)=-\frac{\partial[F(r,p,t)w(r,p,t)]}{\partial p}. \tag{B8}$$

We recognize a continuity equation as Eq. (1) with the force given by

$$F(r,p,t)=\mathrm{Im}\left[W_{21}^{0}(r,p,t)\sum_{\mathrm{L}}\hbar k_{\mathrm{L}}\Omega_{\mathrm{L}}^{*}(r,t)\right]. \tag{B9}$$

So, in a classical picture, this expression of the force shall be used to calculate individual particles trajectories.

The evolution of the Wigner function is given by Eqs. (B3)–(B6), with $W_{ij}(r,p,t)\approx W_{ij}^{0}(r,p,t)w(r,p,t)$, to obtain

$$\frac{\partial W_{11}^{0}(r+pt/m,p,t)}{\partial t}=-\sum_{\mathrm{L}}\mathrm{Im}\big[\Omega_{\mathrm{L}}^{*}(r+pt/m,t)W_{21}^{0}(r+pt/m,p,t)\big], \tag{B10}$$

$$\frac{\partial W_{21}^{0}(r+pt/m,p,t)}{\partial t}=\frac{1}{2i}\sum_{\mathrm{L}}\Omega_{\mathrm{L}}(r+pt/m,t)\big[W_{22}^{0}(r+pt/m,p,t)-W_{11}^{0}(r+pt/m,p,t)\big], \tag{B11}$$

$$\frac{\partial W_{22}^0(r+pt/m,\,p,\,t)}{\partial t} = \sum_{\mathrm{L}} \mathrm{Im}\big[\Omega_{\mathrm{L}}^*(r+pt/m,\,t)W_{21}^0(r+pt/m,\,p,\,t)\big], \tag{B12}$$

where we have used $[\frac{\partial}{\partial t} + \frac{p}{m}\frac{\partial}{\partial r}]W_{11}^0(r+pt/m,\,p,\,t) = \frac{\partial W_{11}^0(r+pt/m,p,t)}{\partial t}$.

We partially recognize the optical Bloch equations [Eq. (B1)], with $\sigma_{ij}(t) = W_{ij}^0(r_0 + p_0 t/m,\, p_0,\, t)$ [20]. This is the usual first order in time connection between Lagrangian and Eulerian specification: $\boldsymbol{r}(t) = \boldsymbol{r}(t; \boldsymbol{r}_0, \boldsymbol{v}_0, t_0) \approx r_0 + v_0 t,\ p(t) \approx p_0$. So to first order $\sigma_{ij}(t) \approx W_{ij}^0(r(t),\, p(t),\, t)$ and the force given by Eq. (B9) is exactly the same force as Eq. (B2).

An alternative way to derive these expressions consists in using the interaction picture. A similar method using $w^I(r,\,p,\,t) = W_{11}^I + W_{22}^I W_{ij}^I(r,\,p,\,t) \approx {W_{ij}^I}^0(r,\,p,\,t)w(r,\,p,\,t)$ from Eqs. (A13)–(A15) leads, to first order in $\hbar k_{\mathrm{L}}$, to

$$\frac{\partial {W_{11}^I}^0}{\partial t}(r,\,p,\,t) = -\sum_{\mathrm{L}} \mathrm{Im}\big[\Omega_{\mathrm{L}}^*(r,\,p,\,t){W_{21}^I}^0(r,\,p,\,t)\big], \tag{B13}$$

$$\frac{\partial {W_{21}^I}^0}{\partial t}(r,\,p,\,t) = \frac{1}{2i}\sum_{\mathrm{L}} \Omega_{\mathrm{L}}(r,\,p,\,t)\big[{W_{22}^I}^0(r,\,p,\,t) - {W_{11}^I}^0(r,\,p,\,t)\big], \tag{B14}$$

$$\frac{\partial {W_{22}^I}^0}{\partial t}(r,\,p,\,t) = \sum_{\mathrm{L}} \mathrm{Im}\big[\Omega_{\mathrm{L}}^*(r,\,p,\,t){W_{21}^I}^0(r,\,p,\,t)\big], \tag{B15}$$

which are the usual Bloch equations in the particle frame. The Doppler effect is here explicitly included. Indeed, the continuity equation reads as

$$\frac{\partial w^I}{\partial t}(r,\,p,\,t) = -\left[-\frac{t}{m}\frac{\partial}{\partial r} + \frac{\partial}{\partial p}\right][F^I(r,\,p,\,t)w^I(r,\,p,\,t)]$$

for the force $F(\boldsymbol{r} + \boldsymbol{p}t/m,\, \boldsymbol{p},\, t) = F^I(r,\,p,\,t) = \sum_{\mathrm{L}} \hbar k_{\mathrm{L}} \Omega_L^*(r,\,p,\,t)W_{21}^I(r,\,p,\,t)^0$.

This is indeed the classical continuity equation (1). In the interaction picture $\rho(\boldsymbol{r},\,\boldsymbol{p},\,t) = \rho^I(\boldsymbol{r} - \boldsymbol{p}t/m,\,\boldsymbol{p},\,t)$ leads to

$$\frac{\partial \rho^I}{\partial t}(\boldsymbol{r},\,\boldsymbol{p},\,t) + \left[-\frac{t}{m}\frac{\partial}{\partial \boldsymbol{r}} + \frac{\partial}{\partial \boldsymbol{p}}\right](\rho^I F^I)(\boldsymbol{r},\,\boldsymbol{p},\,t) = 0, \tag{B16}$$

where $F(\boldsymbol{r},\,\boldsymbol{p},\,t) = F^I(\boldsymbol{r} - \boldsymbol{p}t/m,\,\boldsymbol{p},\,t)$.

APPENDIX C: QUANTITATIVE DEFINITION OF THE PSD

We define the different quantities related to the generic term phase-space density (PSD) and position-momentum distribution (PMD) that are used in the main text as follows.

(i) The PMD are functions of position r and momentum p.

(ii) The PSD are single values that are used to characterize how cold and dense the system is.

The PSD quantities can be arranged in two main categories.

(1) Position-momentum based PSD are simply the maximum of the PMD functions (such as the Wigner or Husimi distributions).

(2) Entropy based PSD are the value $D = e^{-S}$ for a given entropy definition S. The entropies are defined using the density matrix $\hat{\rho}$. They are of the following two types.

(i) Informational (or population-based, or diagonal) PSD: based on the populations $p_i = \langle i|\hat{\rho}|i\rangle$ of specific states $|i\rangle$ (usually a complete basis set) chosen for their physical interest.

(ii) Eigenvalues (or spectral) PSD: based on eigenvalues λ_i of the density matrix $\hat{\rho}$.

The PSD can include or not the following internal states.

(i) For the full system, the PSD is calculated from the whole density matrix of the full particle system AB ($\hat{\rho} = \hat{\rho}_{AB}$), where A and B denote the subspaces related to the external and internal degrees of freedom, respectively. Note that a quantification of the optical field would require a dedicated extra subspace C ($\hat{\rho} = \hat{\rho}_{ABC}$).

(ii) For the position-momentum only (part A), we are interested in the degrees of external freedom, i.e., the coordinates r, p regardless of the internal state. Thus the total density matrix is replaced by the partial density matrix obtained by tracing out the B part: $\hat{\rho}_A = \mathrm{Tr}_B\hat{\rho}$. For instance, with a two-level particle and a $|p, g\rangle$ or $|p, e\rangle$ basis, $\langle p|\hat{\rho}_A(t)|p'\rangle = \langle p, g|\hat{\rho}(t)|p', g\rangle + \langle p, e|\hat{\rho}(t)|p', e\rangle$.

1. Position momentum distribution

The usual Wigner function $W = W_{gg} + W_{ee}$, as plotted in Fig. 2(c), is given by Eq. (A3) with

$$W_{gg}(\boldsymbol{r},\,\boldsymbol{p},\,t) = \frac{1}{h^3}\int \langle \boldsymbol{p} - \boldsymbol{p}'/2,\, g|\hat{\rho}|\boldsymbol{p} + \boldsymbol{p}'/2,\, g\rangle e^{-i\boldsymbol{r}\cdot\boldsymbol{p}'/\hbar} d\boldsymbol{p}' \tag{C1}$$

and an equivalent expression for the excited state W_{ee}.

A smoothed version is obtained by averaging Eq. (C1) over an equivalent cell area of $2\pi\sigma_r\sigma_p$ weighted by a Gaussian function, which corresponds to the so-called Weierstrass transform (in 1D):

$$W_G\sigma_r, \sigma_p(r,\,p) = \int dr'dp' W(r,\,p)G_{\sigma_r,\sigma_p}(r, r';\, p,\, p'),$$

where $G_{\sigma_r,\sigma_p}(r,r';p,p') = \frac{2}{h}e^{(-\frac{(r-r')^2}{2\sigma_r^2}-\frac{(p-p')^2}{2\sigma_p^2})}$. $W_{\sigma_r,\sigma_p}(r,p)$ represents a probability resulting from simultaneous measurement of position and momentum. The uncertainties are σ_r and σ_p as also used in this work [70–74]. The Q-Husimi distribution is a special case with a minimal equivalent cell area of $h/2$ occurring when $\sigma_r\sigma_p = \hbar/2$. This is the optimal distribution obtained for joint position and momentum measurement [75]. The Husimi function is defined and positive and is equal to the average of the density operator over a coherent state $|\alpha(r,p) = \frac{r}{\sigma_r} + i\frac{p}{\sigma_p}\rangle$. So, $Q(r,p,t) = \frac{1}{\pi}\langle\alpha|\hat{\rho}_A|\alpha\rangle$ is the probability distribution of a heterodyne measurement performed on the state $|\alpha\rangle$ [76]. $Q(r,p,t) = Q_{gg}(r,p,t) + Q_{gg}(r,p,t) = \frac{1}{\pi}(\langle\alpha,g|\hat{\rho}|\alpha,g\rangle + \langle\alpha,e|\hat{\rho}|\alpha,e\rangle)$ is the function plotted in Fig. 2(d). Its maximum is plotted in Fig. 3.

2. Informational phase-space density

Several states $|i\rangle$ can be used to define an informational PSD, such as energy states $|E_i\rangle$, momentum states $|p\rangle$, or also coherent states $|\alpha(r,p)\rangle$. For instance, if only the external degrees of freedom (subspace A) are of interest, the energy eigenstates are $E_p = \boldsymbol{p}^2/2m$ for free particles and $E_n = \hbar\omega(n+1/2)$ for 1D harmonically trapped particles. If, on the other hand, the full system AB is considered, the internal energy must be added.

Several definitions of PSD are possible depending of the choice of the function of the parameters $\mathcal{F}(p_i)$ (see discussion below). An important one is the (Gibbs-)Shanon entropy $S_{\rm Sh} = -\sum_i p_i \ln p_i$. So, for the full space AB,

$$S_{\rm Sh} = -\Bigg[\sum_p \langle p,g|\hat{\rho}|p,g\rangle \ln(\langle p,g|\hat{\rho}|p,g\rangle) + \sum_p \langle p,e|\hat{\rho}|p,e\rangle \ln(\langle p,e|\hat{\rho}|p,e\rangle)\Bigg], \quad \text{(C2)}$$

while, for the external degrees of freedom only,

$$S_{\rm Sh}^{\{A\}} = -\sum_p [\langle p,g|\hat{\rho}(t)|p,g\rangle + \langle p,e|\hat{\rho}(t)|p,e\rangle] \times \ln[\langle p,g|\hat{\rho}(t)|p,g\rangle + \langle p,e|\hat{\rho}(t)|p,e\rangle]. \quad \text{(C3)}$$

Finally, considering a specific internal state only, e.g., the ground state, it can be also defined as

$$S_{\rm Sh}^{(g)} = -\sum_p \langle p,g|\hat{\rho}|p,g\rangle \ln(\langle p,g|\hat{\rho}|p,g\rangle). \quad \text{(C4)}$$

3. Spectral phase-space density

The spectral PSD can be seen as a special case of population entropy when the states $|i\rangle$ are the eigenstates of the density matrix, i.e., $p_i = \lambda_i$. This gives rise to another definition of PSD known as the Von Neumann entropy $S_{\rm VN} = -\sum_i \lambda_i \ln(\lambda_i)$. Such a definition has the advantage of being independent of the basis choice and is unambiguously defined from the density matrix as $S_{\rm VN} = -{\rm Tr}[\hat{\rho}\,\ln(\hat{\rho})]$. The related PSD $D_{\rm VN} = e^{-S_{\rm VN}}$ was plotted for the full density matrix in Fig. 3(a) and the partial density matrix in Fig. 3(b). The possible modification of $S_{\rm VN}^{\{A\}}$ is obviously linked to the mutual entropy $S_{\rm VN}^{\{A\}} + S_{\rm VN}^{\{B\}} - S_{\rm VN}^{\{AB\}}$ defining the maximal cooling (work) that can be achieved in quantum thermodynamics [22]. The triangle inequality Eq. (6) indicates that a subtly correlated system could even lead to an increase of $D_{\rm VN}^{\{A\}}$ by a factor M^2 [26]. However, under the canonical conditions where only one internal state is populated, the gain of $D_{\rm VN}^{\{A\}}$ is bounded to M since $S_{\rm VN}^{\{AB\}}(0) = S_{\rm VN}^{\{A\}}(0)$ and $S_{\rm VN}^{\{AB\}}(t) = S_{\rm VN}^{\{AB\}}(0)$. This is consistent with the results shown in Fig. 3(b), where the gain on $D_{\rm VN}^{\{A\}}$ is greater than one but lower than $M = 2$.

4. Other entropy definitions

Other functions $\mathcal{F}$ of the parameters can be used to define the entropy. For instance, power function leads to Tsallis entropy: $S_q = \frac{1}{q-1}[1 - \sum_i p_i^q]$. For $q \to 1$, it reduces to the Shanon entropy and for $q \to \infty$ to the maximal population of $\hat{\rho}$.[2]

Combining with logarithmic function leads to the Rényi entropy $S_R^{(q)} = \frac{1}{1-q}\log[\sum_i p_i^q]$. The case $q = 0$ is the Hartley or max entropy, $q \to 1$ is the Shannon entropy, $q = 2$ is the collision or simply called Rényi entropy, and $q \to \infty$ the min entropy.

It is important to realize that, for a given choice of $\mathcal{F}$, a given PSD will have a population version $\mathcal{F}(p_i)$ but also an eigenvalue one (when $p_i = \lambda_i$). Sometimes, the terminology is ambiguous and it is important to be precise if a function of p_i or λ_i is used. Fortunately, some definitions are not ambiguous; for instance, the Von Neumann entropy is always an eigenvalue function. The Von Neumann entropy is therefore always the Shannon entropy over the spectrum of $\hat{\rho}$. Similarly the so-called (Tsallis-2) linear entropy (because it approximates the Von Neumann entropy when $\ln\hat{\rho} \approx \hat{\rho} - 1$ [77]) $S_L = 1 - \sum_i \lambda_i^2 = 1 - {\rm Tr}(\hat{\rho}^2)$ is usually used over the spectrum of $\hat{\rho}$ because it quantifies the purity of the quantum state [purity being defined by ${\rm Tr}(\hat{\rho}^2)$ [2,78]].

5. Relation between PSD and PMD

The function $\mathcal{F}$ can also be used to define a single value PSD from a PMD. For instance, we can define the so-called Wehrl entropy $S_W = -\int Q(r,p)\ln Q(r,p)\,dr\,dp$. This is a continuous (or differential) entropy in which $Q(r,p)$ is seen as a probability density function. Wehrl's entropy is the classical limit $h \to 0$ of the Von Neumann quantum entropy [79].

The linear entropy could also be used because, compared to other definitions of the entropy, it has the direct Weyl-Wigner-Moyal transcription: $S_R = 1 - {\rm Tr}(\hat{\rho}_A^2) = 1 - h\int W(r,p)^2\,dr\,dp$ (so-called Manfredi-Feix entropy) [77,80,81].

6. Relation and bounds between PSD

a. Informational versus spectral PSD

An informational entropy is always larger than the corresponding spectral entropy.

---

[2]Because $\lim_{q\to\infty}\|\cdot\|_q = \|\cdot\|_\infty$, that is $\lim_{q\to\infty}(\sum_i |p_i|^q)^{1/q} = \max_i p_i$.

The key argument is based on the Schur-Horn theorem (that indicates essentially that $p_i \leqslant \lambda_i$) and on the fact that the functions $\mathcal{F}$ are concave (as the power or logarithmic functions) in order to keep some basic properties of the entropies such as increasing with disorder. Then Jensen's inequality for concave function proves the result [22–25,76,82,83].

For instance, $\mathcal{F}(x) = -x\ln(x)$ leads to $S_{\rm Sh} \geqslant S_{\rm VN}$ (or equivalently $D_{\rm Sh} \leqslant D_{\rm VN}$).

b. Invariance of full PSD

The invariance of the full eigenvalues PSD is obvious using series of $\mathcal{F}(x)$, the unitarity of the evolution operator $\hat{U}$ [$\hat{\rho}(t) = \hat{U}(t)\hat{\rho}(0)\hat{U}^\dagger$], and the cyclic invariant of the trace. The fact that all functions of the eigenvalues λ_i are conserved is the argument used in Ref. [1] to show that the min-entropy $S_\infty = -\log\max_i \lambda_i = -\log\|\hat{\rho}\|_\infty$ or the spectral radius $D_\infty = \|\hat{\rho}\|_\infty = \max_i(\lambda_i)$ of $\hat{\rho}$ (maximum occupation number of quantum eigenstates λ_i) are conserved under Hamiltonian evolution (and so that the related PSD cannot vary).

c. Bound by the number of internal states M

The evolution operator $\hat{U}$ can also be used to demonstrate other bounds [2] such as

$$\max[\hat{\rho}_A(t)] \leqslant M\ \max[\hat{\rho}_A(0)]. \tag{C5}$$

This is demonstrated by considering $\max_p[\langle p|\hat{\rho}_A(t)|p\rangle] = \sum_{i=1}^{M}\langle p_0, i|\hat{\rho}(t)|p_0, i\rangle$ in addition to $\langle p_0, i|\hat{\rho}(t)|p_0, i\rangle = \sum_{p,j} U_{p_0 i, pj}\rho_{pj,pj}(0)U^*_{pj,p_0 i} \leqslant \max[\hat{\rho}_A(0)]\sum_{p,j} U_{p_0 i, pj}U^*_{pj,p_0 i} \leqslant \max[\hat{\rho}_A(t)]$ that arises from the unitarity of the evolution operator $\hat{U}$.

In a similar manner [using $\mathcal{F}(x) = x^n$ and $\lim_{n\to\infty}\|\cdot\|_n = \|\cdot\|_\infty$ with the theorem (5) of [76]] it can be shown (see also [76]) that the Husimi function Q and the Wehrl entropy are bounded by the same factor M. More detail and other bounds can be found in Refs. [22–25,76,82,83].

As an important final precaution, again we mention that using pseudo-phase-space-density definitions, as the ones filtering a specific state [such as the ground state only $S^{(g)}_{\rm Sh} = -\sum_p\langle p, g|\hat{\rho}|p, g\rangle\ln(\langle p, g|\hat{\rho}|p, g\rangle)$], it is possible to find an increase larger than M. This is because such pseudo PSD are based neither on a properly defined density matrix nor a partial trace of $\hat{\rho}$.

[1] W. Ketterle and D. E. Pritchard, Atom cooling by time-dependent potentials, Phys. Rev. A **46**, 4051 (1992).

[2] A. Bartana, R. Kosloff, and D. J. Tannor, Laser cooling of internal degrees of freedom. II, J. Chem. Phys. **106**, 1435 (1997).

[3] C. Corder, B. Arnold, and H. Metcalf, Laser Cooling without Spontaneous Emission, Phys. Rev. Lett. **114**, 043002 (2015).

[4] J. P. Bartolotta, M. A. Norcia, J. R. K. Cline, J. K. Thompson, and M. J. Holland, Laser cooling by sawtooth-wave adiabatic passage, Phys. Rev. A **98**, 023404 (2018).

[5] G. P. Greve, B. Wu, and J. K. Thompson, Laser cooling with adiabatic transfer on a Raman transition, arXiv:1805.04452.

[6] E. Korsunsky, Laser cooling during velocity-selective adiabatic population transfer, Phys. Rev. A **54**, R1773 (1996).

[7] C. Corder, B. Arnold, X. Hua, and H. Metcalf, Laser cooling without spontaneous emission using the bichromatic force, J. Opt. Soc. Am. B **32**, B75 (2015).

[8] V. S. Ivanov, Y. V. Rozhdestvensky, and K.-A. Suominen, Theory of robust subrecoil cooling by stimulated Raman adiabatic passage, Phys. Rev. A **85**, 033422 (2012).

[9] H. Metcalf, Entropy exchange in laser cooling, Phys. Rev. A **77**, 061401 (2008).

[10] H. Metcalf, Colloquium: Strong optical forces on atoms in multifrequency light, Rev. Mod. Phys. **89**, 041001 (2017).

[11] M. A. Norcia, J. R. K. Cline, J. P. Bartolotta, M. J. Holland, and J. K. Thompson, Narrow-line laser cooling by adiabatic transfer, New J. Phys. **20**, 023021 (2018).

[12] B. R. Mollow, Pure-state analysis of resonant light scattering: Radiative damping, saturation, and multiphoton effects, Phys. Rev. A **12**, 1919 (1975).

[13] C. Cohen-Tannoudji, J. Dupont-Roc, and G. Grynberg, *Photons and Atoms - Introduction to Quantum Electrodynamics* (Wiley-Interscience, New York, 1997).

[14] J. Dalibard, Une brève histoire des atomes froids (les réseaux optiques et le refroidissement par bande latérale), lecture notes in College de France, 2015 (unpublished).

[15] D. J. Evans and D. J. Searles, The fluctuation theorem, Adv. Phys. **51**, 1529 (2002).

[16] A. K. Pattanayak, D. W. C. Brooks, A. de La Fuente, L. Uricchio, E. Holby, D. Krawisz, and J. I. Silva, Coarse-grained entropy decrease and phase-space focusing in Hamiltonian dynamics, Phys. Rev. A **72**, 013406 (2005).

[17] P. H. Chavanis and F. Bouchet, On the coarse-grained evolution of collisionless stellar systems, Astron. Astrophys. **430**, 771 (2005).

[18] K. Floettmann, Some basic features of the beam emittance, Phys. Rev. Spec. Top. Accel. Beams **6**, 34202 (2003).

[19] O. Steuernagel and H. Paul, Decoherence from spontaneous emission, Phys. Rev. A **52**, R905 (1995).

[20] J. Dalibard and C. Cohen-Tannoudji, Atomic motion in laser light: Connection between semiclassical and quantum descriptions, J. Phys. B **18**, 1661 (1985).

[21] T. Curtright, D. B. Fairlie, and C. K. Zachos, *A Concise Treatise on Quantum Mechanics in Phase Space* (World Scientific, Singapore, 2014).

[22] S. Vinjanampathy and J. Anders, Quantum thermodynamics, Contemp. Phys. **57**, 545 (2016).

[23] E. Boukobza and D. J. Tannor, Entropy exchange and entanglement in the Jaynes-Cummings model, Phys. Rev. A **71**, 063821 (2005).

[24] I. Bengtsson and K. Życzkowski, *Geometry of Quantum States: An Introduction to Quantum Entanglement* (Cambridge University Press, Cambridge, UK, 2017).

[25] J. Gemmer, M. Michel, and G. Mahler, *Quantum Thermodynamics–Emergence of Thermodynamic Behavior Within Composite Quantum Systems*, 2nd ed., Lecture Notes in Physics (Springer, Berlin, 2009).

[26] M. N. Bera, A. Riera, M. Lewenstein, and A. Winter, Generalized laws of thermodynamics in the presence of correlations, Nat. Commun. **8**, 2180 (2017).

[27] N. V. Vitanov, A. A. Rangelov, B. W. Shore, and K. Bergmann, Stimulated Raman adiabatic passage in physics, chemistry, and beyond, Rev. Mod. Phys. **89**, 015006 (2017).

[28] P. V. Pyshkin, D.-W. Luo, J. Q. You, and L.-A. Wu, Ground-state cooling of quantum systems via a one-shot measurement, Phys. Rev. A **93**, 032120 (2016).

[29] A. M. Jayich, A. C. Vutha, M. T. Hummon, J. V. Porto, and W. C. Campbell, Continuous all-optical deceleration and single-photon cooling of molecular beams, Phys. Rev. A **89**, 023425 (2014).

[30] D. Comparat, Molecular cooling via Sisyphus processes, Phys. Rev. A **89**, 043410 (2014).

[31] M. E. Carrera-Patino and R. S. Berry, Entropy production in stopping atoms with laser light, Phys. Rev. A **34**, 4728 (1986).

[32] S. J. D. Phoenix and P. L. Knight, Fluctuations and entropy in models of quantum optical resonance, Ann. Phys. (N.Y.) **186**, 381 (1988).

[33] X.-Q. Yan and Y.-G. Lü, A condition for entropy exchange between atom and field, Commun. Theor. Phys. **57**, 209 (2012).

[34] X.-Q. Yan, B. Shao, and J. Zou, Entropy exchange and entanglement of an in motion two-level atom with a quantized field, Chaos Solitons Fractals **37**, 835 (2008).

[35] S. Xie, F. Jia, and Y. Yang, Dynamic control of the entanglement in the presence of the time-varying field, Opt. Commun. **282**, 2642 (2009).

[36] M. S. Ateto, Quantum entropy of a nonlinear two-level atom with atomic motion, Int. J. Theor. Phys. **49**, 276 (2010).

[37] N. Zidan, Partial entropy creation of a two-level atom with intrinsic decoherence, Physica A (Amsterdam) **391**, 401 (2012).

[38] E. M. Khalil, Influence of the external classical field on the entanglement of a two-level atom, Int. J. Theor. Phys. **52**, 1122 (2013).

[39] S. J. van Enk and G. Nienhuis, Entropy production and kinetic effects of light, Phys. Rev. A **46**, 1438 (1992).

[40] X. L. Ruan, S. C. Rand, and M. Kaviany, Entropy and efficiency in laser cooling of solids, Phys. Rev. B **75**, 214304 (2007).

[41] A. Beige, P. L. Knight, and G. Vitiello, Cooling many particles at once, New J. Phys. **7**, 96 (2005).

[42] G. Vacanti and A. Beige, Cooling atoms into entangled states, New J. Phys. **11**, 083008 (2009).

[43] M. G. Raizen, J. Koga, B. Sundaram, Y. Kishimoto, H. Takuma, and T. Tajima, Stochastic cooling of atoms using lasers, Phys. Rev. A **58**, 4757 (1998).

[44] V. I. Balykin and V. S. Letokhov, Informational cooling of neutral atoms, Phys. Rev. A **64**, 063410 (2001).

[45] V. Vuletić and S. Chu, Laser Cooling of Atoms, Ions, or Molecules by Coherent Scattering, Phys. Rev. Lett. **84**, 3787 (2000).

[46] M. Gangl, P. Horak, and H. Ritsch, Cooling neutral particles in multimode cavities without spontaneous emission, J. Mod. Opt. **47**, 2741 (2000).

[47] K. Murr, Large Velocity Capture Range and Low Temperatures with Cavities, Phys. Rev. Lett. **96**, 253001 (2006).

[48] J.-H. Chen and H.-Y. Fan, Entropy evolution law in a laser process, Ann. Phys. (N.Y.) **334**, 272 (2013).

[49] C. Cohen-Tannoudji, J. Dupond-Roc, and G. Grynberg, *Processus d'Interaction entre Photons et Atomes* (InterEdition, Paris, 1988).

[50] S. M. Barnett and M. Sonnleitner, Vacuum friction, J. Mod. Opt. **65**, 706 (2018).

[51] M. Sonnleitner and S. M. Barnett, The Roentgen interaction and forces on dipoles in time-modulated optical fields, Eur. Phys. J. D **71**, 336 (2017).

[52] S. M. Yoo and J. Javanainen, Wigner-function approach to laser cooling in the recoil limit, J. Opt. Soc. Am. B **8**, 1341 (1991).

[53] H.-W. Lee, Theory and application of the quantum phase-space distribution functions, Phys. Rep. **259**, 147 (1995).

[54] K. Takahashi, Distribution functions in classical and quantum mechanics, Prog. Theor. Phys. Suppl. **98**, 109 (1989).

[55] C. C. Martens, A. Donoso, and Y. Zheng, Quantum trajectories in phase space, in *Quantum Trajectories*, 1st ed., edited By P. Kumar Chattaraj (CRC Press, Boca Raton, 2010), Chap. 7, p. 95.

[56] R. E. Wyatt, *Quantum Dynamics with Trajectories: Introduction to Quantum Hydrodynamics* (Springer Science & Business Media, New York, 2006), Vol. 28.

[57] P. K. Chattaraj, *Quantum Trajectories* (CRC Press, Boca Raton, FL, 2016).

[58] X. Hua, C. Corder, and H. Metcalf, Simulation of laser cooling by the bichromatic force, Phys. Rev. A **93**, 063410 (2016).

[59] C. Cohen-Tannoudji, Atomic motion in laser light, Fund. Syst. Quantum Opt. **53**, 1 (1990).

[60] H. J. Metcalf and P. van der Straten, *Laser Cooling and Trapping* (Springer, New York, 1999).

[61] V. I. Romanenko and N. V. Kornilovska, Atoms in the counter-propagating frequency-modulated waves: Splitting, cooling, confinement, Eur. Phys. J. D **71**, 229 (2017).

[62] L. Podlecki, R. Glover, J. Martin, and T. Bastin, Radiation pressure on a two-level atom: An exact analytical approach, J. Opt. Soc. Am. B **35**, 127 (2018).

[63] M. Sonnleitner, N. Trautmann, and S. M. Barnett, Will a Decaying Atom Feel a Friction Force? Phys. Rev. Lett. **118**, 053601 (2017).

[64] V. G. Minogin and V. S. Letokhov, *Laser Light Pressure on Atoms* (CRC Press, Boca Raton, FL, 1987).

[65] A. P. Kazantsev, G. I. Surdutovich, and V. P. Yakovlev, *Mechanical Action of Light on Atoms* (World Scientific, Singapore, 1990).

[66] S. Stenholm, The semiclassical theory of laser cooling, Rev. Mod. Phys. **58**, 699 (1986).

[67] A. V. Bezverbnyi, O. N. Prudnikov, A. V. Taichenachev, A. M. Tumaikin, and V. I. Yudin, The light pressure force and the friction and diffusion coefficients for atoms in a resonant nonuniformly polarized laser field, Sov. JETP **96**, 383 (2003).

[68] O. N. Prudnikov, A. S. Baklanov, A. V. Taichenachev, A. M. Tumaikin, and V. I. Yudin, Kinetics of atoms in a bichromatic field, Sov. JETP **117**, 222 (2013).

[69] V. G. Minogin and Yu. V. Rozhdestvensky, Dynamics of a three-level atom in a resonant light field, Appl. Phys. B: Lasers Opt. **34**, 161 (1984).

[70] V. I. Tatarskiĭ, Reviews of topical problems: The Wigner representation of quantum mechanics, Sov. Phys. Usp. **26**, 311 (1983).

[71] S. Olivares, Quantum optics in the phase space. A tutorial on Gaussian states, Eur. Phys. J. Spec. Top. **203**, 3 (2012).

[72] A. Monras, Phase space formalism for quantum estimation of Gaussian states, arXiv:1303.3682.

[73] T. Ranaivoson, R. Andriambololona, R. Hanitriarivo, and R. Raboanary, Study on a phase space representation of quantum theory, Int. J. Latest Res. Sci. Technol. **2**, 26 (2013).

[74] S. Machnes, E. Assémat, H. R. Larsson, and D. J. Tannor, Quantum dynamics in phase space using projected von Neumann bases, J. Phys. Chem. A **120**, 3296 (2016).

[75] A. S. Roy and S. M. Roy, Optimum phase space probabilities from quantum tomography, J. Math. Phys. **55**, 012102 (2014).

[76] G. D. Palma, The Wehrl entropy has Gaussian optimizers, Lett. Math. Phys. **108**, 97 (2018).

[77] J. J. Włodarz, Entropy and Wigner distribution functions revisited, Int. J. Theor. Phys. **42**, 1075 (2003).

[78] D. J. Tannor and A. Bartana, On the interplay of control fields and spontaneous emission in laser cooling, J. Phys. Chem. A **103**, 10359 (1999).

[79] G. P. Beretta, On the relation between classical and quantum-thermodynamic entropy, J. Math. Phys. **25**, 1507 (1984).

[80] G. Manfredi and M. R. Feix, Entropy and Wigner functions, Phys. Rev. E **62**, 4665 (2000).

[81] P. Sadeghi, S. Khademi, and A. H. Darooneh, Tsallis entropy in phase-space quantum mechanics, Phys. Rev. A **86**, 012119 (2012).

[82] M. Sebawe Abdalla, A.-S. F. Obada, E. M. Khalil, and S. I. Ali, The influence of phase damping on a two-level atom in the presence of the classical laser field, Laser Phys. **23**, 115201 (2013).

[83] C. Werndl and R. Frigg, Entropy–A guide for the perplexed, in *Probabilities in Physics*, edited by C. Beisbart and S. Hartmann (Oxford University Press, Oxford, UK, 2011), pp. 115–142.